AN APPROACH FOR MODELING THE PERFORMANCE OF THERMAL BUBBLE PUMP

Ass.Prof. Dr. Abdulwadood Salman Shihab , Dr. Safaa Hameed Faisal
Foundation of Technical Education, Basrah Technical College

ABSTRACT :

This study suggests a new theoretical analysis for the thermal bubble pump system. The main application of this system is to replace the mechanical pump in vapor absorption refrigeration system. The analysis is based on utilizing one-dimensional slug flow model to describe the void fraction in the riser tube of the pump, and adopting an appropriate method to evaluate the two-phase frictional pressure drop. The model is capable to predict the maximum pumping capacity of the pump in terms of the operation and configuration parameters. Three tube diameters (6.5,10, and 14mm) with four submergence ratios (0.5, 0.6, 0.7, and 0.8) were experienced using water as a working fluid. Results indicate that the maximum pumping capacity is positively increased with increasing the submergence ratio and tube diameter at a fixed riser tube length. The maximum pumping capacity is found to be independent of the liquid temperature at the inlet to the generator under the assumption of stable operation of the pump. It is obtained that the slip ratio decreases with the increasing of the submergence ratio and slightly decrease with the decreasing of the tube diameter.

Key words: Bubble pump, Vapor lift, Two-phase flow, Slug model, void fraction

نهج لنمذجة أداء المضخة الفقاعية الحرارية

الخلاصة

تقترح الدراسةِ تحليلا نظريا جديدا لمنظومة المضخّة الفقاعيةِ الحراريةِ. إنّ التطبيقَ الرئيسيَ للمنظومة يكمن فيْ اَستبدالَ المضخّةَ الميكانيكيةَ في منظومة التبريدِ الامتصاصية. يستند التحليلَ على استخدام نموذج جريان تكتلي أحادي البعدِ لتَمْثيل الكسرِ الفراغي في أنبوب المضخةَ ويَتبنّى طريقةَ ملائمةَ لتَقييم هبوطِ الضغطِ الاحتكاكي في الجريان ثنائي الطور. إنّ النموذجَ قادر على التنبؤِ بسعة الضخّ القصوى للمضخّةِ كدالة للمتغيرات التشغيلية والشكلية للمضخة. تم اختبار أداء المضخة باستخدام الماء كمائع للتشغيل واعتماد ثلاثة أقطار (10،6.5، و 14 مليمتر) بنِسَبِ غطسِ أربع (0.5، 0.6، 0.7، و0.8). تُشيرُ النَتائجُ بأنّ قدرةَ الضخّ القصوى تُزدادُ إيجابياً بزيادة نسبةِ الغطسَ وقطرَ الأنبوب بثْبّوت طولَ إلا نبوب، كما بينت النتائج أيضا أن قدرة الضخّ القصوى كَانتْ مستقلة عن درجةَ حرارة الماء عند دخوله إلى مولّدِ البخار بفرض إن عمليةِ الضخ مستقرّةِ. لقد وجد أن نسبةَ الانزلاق المتَوقّعة من النموذجِ الرياضي تقل مع زيادة نسبةِ الغطسَ و تقل بعض الشّيء مع تقليل قطرِ الأنبوب.

Nomenclatures:

***English Symbols*:**

A:Area(m^2).
$B_{1,2,3}$: Coefficients in eq.(13).
Bo: Bond number=$\left(((\rho_L-\rho_g).g.D_{ris}{}^2)/\sigma_L\right)$.
c: Specific heat(kJ/kg.K))
D: Diameter (m)
Fr: Froude number =$\left(G_{tot}/(gD_{ris}\rho_h{}^2)\right)$
f: Friction factor
G: Mass Flux= $\dot{m}$/A (kg/m^2.s)
g: Gravity(m/s^2)
h: Enthalpy(kJ/kg).
j: Superficial velocity(m/s).
L: Length(m).
$\dot{m}$: Mass flow rate(kg/s)
N_f :The dimensionless inverse viscosity.
P: Pressure(Pa)
Q: Heat power(W).
Re: Reynolds number $=((\rho.u.D)/\mu)$.
R_{subm}: Submergence ratio $=Z_d/L_{ris}$.
S: Slip ratio.
T: Temperature(K).
t: Time(s).
U: Velocity(m/s).
U_o: Taylor bubble rise velocity in a stagnant liquid (m/s).
V : Volume (m^3).
$\dot{V}$: Volume flow rate (m^3/s).
We: Weber number=$\left((G_{tot}{}^2 D_{ris})/(\rho_h\sigma_L)\right)$.
x: Dryness fraction(kg_g/kg_{tot}).
Z: Height(m).
Z_d: Driving head(m).

***Greek Symbols*:**

ρ: Density (kg/m^3).
v: Specific Volume (m^3/kg).
Δ: Difference
ϕ^2: Two phase multiplier
κ: pipe roughness(m)
$\lambda_{1,2}$: Parameters in eq.(10).
α: Void fraction.
μ: Viscosity(kg/m.s).
σ: Surface tension(N/m)
β: Taylor bubble fraction length.
Γ: Parameter in eq.(32).
ω: Parameter in eq.(33).
δ: Liquid film thickness(m).
τ: Shear force(kg/m^2).

Subscripts

0,1,2**:** State point numbers.
*atm***:** Atmospheric**.**
*film***:** Liquid film**.**
*fri***:** Frictional**.**
*GO***:** Gas overall**.**
gen: Generator
*g***:** Gas**.**
*gra***:** Gravitational**.**
*GLS***:** Dispersed gas bubbles in the liquid slug**.**
*h***:** Homogenous**.**
*L***:** Liquid**.**
*LO***:** Liquid overall**.**
*LS***:** Liquid slug**.**
max: Maximum**.**
*ris***:** Riser tube**.**
*sat***:** Saturation state**.**
*SP***:** Single phase**.**
*TB***:** Taylor bubble**.**
*tot***:** Total**.**
*TP***:** Two phase**.**
*u***:** Unit cell**.**
*v***:** Vapor**.**

Abbreviations:

BPVARS:Bubble pump operated vapor absorption refrigeration system.
LiBr: Lithium Bromide
EES: Engineering equation solver.

1.INTRODUCTION:

The bubble pump is merely a vertical tube that does not contain any moving parts and is submerged at its lower part in a liquid to a certain level Fig(1). Heat is applied at the bottom of the tube (the vapor generator) at a rate sufficient to vaporize some of the liquid. The resulting vapor bubbles occupy the cross section of the tub and rises upward. The rising vapor bubble acts like a piston due to its buoyancy force, it lifts a corresponding amount of liquid to the top of the bubble pump (the separator). The main application of vapor-lift pump is to replace the mechanical pump in absorption refrigeration system. This will leads to introduce a fully heat activated refrigeration system.

Delano (1998) studied theoretically and experimentally the vapor bubble pump used in the Einstein diffusion Vapor Absorption Refrigeration System (BPVARS). The Stenning and Martin (1968) model was firstly modified to analyze the performance of the bubble pump. A constant value of 2.5 for the slip ratio was assigned. The theoretical results were correlated to fit the experimental date. Furthermore, the maximum flow rate points were fitted by linear approximation.

Sathe (2001) studied theoretically and experimentally the vapor-lift pump that used for the diffusion BPVARS. The Delano's (1998) methodology was adopted with methyl alcohol as a tested fluid. The fluid pulses out of the bubble pump per unit time were found to increases with increase in the heat input. Moreover, the mass flow rate of vapor increases linearly with the heat input while the pumped liquid mass flow rate first increases, reaches a maximum value and then decreases with the increase in the heat input. The theoretical model predicts lower result from that found experimentally.

Koyfman et al. (2003) carried out an experimental investigation on a closed continuous bubble pump apparatus used for the diffusion BPVARS. The tested fluids were organic solvent as absorbent and hydro-chlorofluorocarbon (R22) as a refrigerant. The results showed that the bubble pump operates at the slug flow regime with a churn flow regime at the entrance of the bubble pump tube.

Zhang et al (2006) carried out an experimental investigations on the performance of the bubble pump with a lunate channel. The proposed bubble pump configuration consist of a small tube locates eccentrically inside a larger one and the whole assembly is mounted inside a bigger diameter pipe. They concluded that a pump with combined diameters ratio of 16/32 mm. is suitable for a refrigerator with cooling capacity of 4.8 kW using heat source temperature of $75^{o}C$.

Vicatos and Bennett (2007) proposed multi tube bubble pump for enhancing the performance of the diffusion BPVARS. The Delano's model (1998) was modified to evaluate the performance of multi tube bubble pump arrangement. It is concluded that the multiple lift tube bubble pump is a viable and workable solution to increase the refrigeration capacity without any change in the coefficient of performance.

Shihab and Morad (2012) performed a theoretical and experimental study on the vapor bubble pump. The Delano's model (1998) was modified and the method that was recommended by Stenning and Martin (1968) was developed to evaluate the frictional pressure drop. Theoretically, it is found that the length of the riser beyond 1.3 m has insignificant effect on its performance. The theoretical prediction of the pumping capacities were lower than the experimental results for all values of tube diameter and submergence ratios. A new K-factor equation was introduced to correlate the theoretical result with the experimental data.

Faisal (2012) studied the performance of LiBr-Water pumpless absorption refrigeration system. A simulated test rig of the thermal bubble pump was fabricated using water as a test fluid. Three tubes diameters were tested 6.5, 10, and 14 mm with riser tube length of 1.5 m. It is found that for fixed generator input temperature of 102 ^{o}C and a riser tube of 10 mm diameter, the pumping capacity reached its maximum of 0.0295 kg/s and 0.043 kg/s for submergence ratios of 0.5 and 0.7 respectively, then the pumping capacity fallen down at higher heat supply. The same trend of the pumping capacity variation with heat input was similar for other riser tub diameters. Experimental

observations showed that the two phase slug flow was dominant at the maximum pumping of the bubble pump while an annular flow appeared beyond the maximum point.

The present study is focused to establish a mathematical model of the bubble pump with two-phase slug flow mechanism relating the pump capacity and its geometrical configuration adopting an approach to evaluate the frictional pressure drop based on general working fluid properties.

2.MODELING APPROACH:

The analytical model is based on the conservation of the mass, momentum, and the energy. It is to predict the pumping capacity for a specified pump configuration and operation parameters. The analysis is introduced for atmospheric thermal bubble pump with water as a working fluid with the following assumptions.

1. Steady state, one-dimensional, incompressible adiabatic flow.
2. The generator produces saturated water and vapor.
3. Negligible pressure drop due to the friction in the pipes and fittings before the vapor generator.

Referring to the fig. (1), applying the mass balance equation from point 1 to point 2 assuming the two-phase mixture at the exit of the generator is homogenous yields (Darby, 2001):

$$\dot{m}_{tot} = \rho_1 A_{gen} U_1 = \rho_h A_{gen} U_2 = \dot{m}_L + \dot{m}_v \quad (1)$$

The homogenous mixture density is given by (Wallis, 1969):

$$\rho_h = \left(\nu_L .(1-x) + \nu_v .x\right)^{-1} \quad (2)$$

Where:

$$x = \dot{m}_v / \dot{m}_{tot} \quad (3)$$

The generator pressure (P_2) is saturated pressure at the generator temperature (T_2):

$$P_2 = P_{sat}(T_2) \quad (4)$$

Appling Bernoulli equation from the liquid surface at the downcomer to point 1 yields (Darby, 2001):

$$P_1 = P_{atm} + \rho_0 g(R_{subm} .L_{ris} + Z_{gen}) - 0.5\rho_1 {U_1}^2 \quad (5)$$

Where R_{subm} is the ratio of driving head (Z_d), to the bubble pump riser length (L_{ris}):

$$R_{subm} = Z_d / L_{ris} \quad (6)$$

By using this dimensionless parameter (R_{subm}), the bubble pump performance can be evaluated regardless the values of the riser and downcomer lengths.

At the generator, heat energy is added to produce vapor with dryness fraction (x). Applying the energy balance for the generator gives (Faisal ,2012):

$$Q_{gen} = \dot{m}_{tot}(h_2 - h_1) \quad (7)$$

$$h_2 = h_L .(1-x) + x.h_v \quad (8)$$

h_L, h_v: are the specific enthalpies of the saturated liquid and saturated vapor respectively at the generator temperature.

Next, applying the conservation of momentum for the generator results in (Darby, 2001):

$$\dot{m}_{tot}(U_2 - U_1) = P_1 A_{gen} - P_2 A_{gen} - \rho_h A_{gen} Z_{gen} g - f(0.5\rho {U_2}^2) Z_{gen} \pi D_{gen} \quad (9)$$

f : The Fanning friction factor given by (Darby, 2001):

$$f = 2\left[\left(\frac{8}{\mathrm{Re}}\right)^{12} + \frac{1}{(\lambda_1 + \lambda_2)^{3/2}}\right]^{1/12} \quad (10)$$

Where:

$$\lambda_1 = \left[2.457 \ln\left(\frac{1}{(7/\mathrm{Re})^{0.9} + 0.27(\kappa/D)}\right)\right]^{16}; \quad \lambda_2 = \left(\frac{37530}{\mathrm{Re}}\right)^{16}; \quad \mathrm{Re} = (D\ .\rho\ .U\ )/\mu$$

A typical value of (κ) is given to be 0.002 mm for a wide range of materials (Darby, 2001).

Actually, the most important challenge for the present model is to represent an expression to calculate the two-phase pressure drop across the riser tube. Determining such expression, the analytical model of the bubble pump will be completed. This can be achieved through expressing the pressure drop to become as the ability of the buoyancy force to overcome the gravitational and friction force of the flowing mixture (Collier & Thome 1994):

$$(P_2 - P_{atm}) = \Delta P_{TP} = \Delta P_{gra} + \Delta P_{fri} \quad (11)$$

The gravitation term represents the weight of the fluids (body force) and the friction term represents the shear force (surface force) at the wall.

Frictional Pressure Drop:

The frictional pressure drop in the two-phase flow has a special treatment. It is usually related with the single-phase pressure drop (ΔP_{SP}) by what is called "Two-Phase Multiplier ϕ^2". The two-phase frictional pressure drop is given by (Collier & Thome 1994):

$$\Delta P_{fri} = \phi^2{}_{LO} . \Delta P_{SP,fri,LO} = \phi^2{}_{GO} . \Delta P_{SP,fri,GO} \quad (12)$$

Where the values of ($\Delta P_{SP,fri,LO}$) and ($\Delta P_{SP,fri,GO}$) are the single-phase frictional pressure drop. The
subscript (*LO*) and (*GO*) refer to assumption that all mass flow rate of the two-phase is assumed to be all-liquid (Liquid Overall) or all-gas (Gas Overall). In this study, the Friedel multiplier is adopted. This multiplier relates the two phase pressure drop with the single-phase pressure drop. It was obtained by optimizing an equation for a large data base of two-phase pressure drop measurements (Collier & Thome 1994):

$${\phi_{LO}}^2 = B_1 + \frac{3.24 B_2 B_3}{Fr^{0.045} We^{0.035}} \quad (13)$$

Where:

$$B_1 = (1-x)^2 + x^2\left(\frac{\rho_L \cdot f_{GO}}{\rho_g \cdot f_{LO}}\right) \;\; ; \;\; B_2 = x^{0.78}(1-x)^{0.224} \;\; ; \;\; B_3 = \left(\frac{\rho_L}{\rho_g}\right)^{0.91}\left(\frac{\mu_g}{\mu_L}\right)^{0.19}\left(1-\frac{\mu_g}{\mu_L}\right)^{0.7}$$

$$We = \frac{G_{tot}{}^2 D_{ris}}{\rho_h \sigma_L} \quad ; \quad Fr = \frac{G_{tot}}{g D_{ris} \rho_h{}^2}$$

The value of the single phase frictional pressure drop ($\Delta P_{SP,\,fri,LO}$) is found as (Darby, 2001):

$$\Delta P_{SP,\,fri,LO} = (2 f_{LO} \nu_L G_{tot}{}^2 L_{ris}) / D_{ris} \tag{14}$$

Where;

D_{ris}: Riser tube diameter

G_{tot}: Total mass flux which is equal to the mass flow rate per unit of cross sectional area.

f_{LO}: The single-phase fanning friction factor that can be calculated using eq.(10).

All fluid properties are found in the EES software packages (Klein & Alvarado, 2004).

Gravitational Pressure Drop:

The gravitational term (ΔP_{gra}) represents the weight of the mixture column in the tube (Collier & Thome 1994):

$$\Delta P_{gra} = \rho_{TP} . g . L_{ris} = [\rho_L (1-\alpha) + \rho_g (\alpha)] . g . L_{ris} \tag{15}$$

Where: (α) is the void Fraction defined as the area of the pipe cross section occupied by the gas to the total riser tube area,(Collier & Thome 1994)i.e:

$$\alpha = A_g / A_{ris} \tag{16}$$

The two phase density (ρ_{TP}) differs from the homogenous density given in eq.(1), where there is no slip between phases, but in the two-phase density, the slip between phases is considered.

In this study, the maximum liquid discharge is expected to take place when the flow pattern is of slug flow; therefore a one-dimensional slug model is adopted to describe the void fraction.

One-Dimensional Slug Flow Model:

In this model, a steady and fully developed slug flow is described as a regular succession of identical unit cells. The unit cell consists of a bullet shaped gas bubble surrounded by a liquid film and attached with a liquid slug as shown in the fig.(2).

In multiphase flow, the large bubble of the lighter phase that formed by coalescence of small bubbles is called "Taylor bubble". The term is named after G. I. Taylor (Wallis, 1969).

The one-dimensional slug flow model is based on the following assumptions:

1. The flow is incompressible with constant properties.
2. The expansion of the Taylor bubbles is negligible.
3. All units move steadily upwards at a constant translation velocity without any deformation.
4. The bullet shaped Taylor bubbles are modeled analytically as cylinders.

The following items represent the necessary formulas for analyzing the one-dimensional slug flow:

Superficial Velocity:

It is the velocity of the flowing phases or it can be defined as the velocity that each phase would have if it occupied the entire area of the pipe alone, i.e (Collier & Thome 1994):

$$j_g = \dot{V}_g / A_{ris} \quad ; \quad j_L = \dot{V}_L / A_{ris} \tag{17}$$

Gas Mass Balance:

From fig.(2), it can be seen that the gas enters the riser continuously at a volume flow rate of ($\dot{V}_g$) and superficial velocity of (j_g). Taking the flow of a unit cell entering at section (*O-O*) and leaves at section ($O'-O'$), the gas flow occurs intermittently in a two forms. These are the long bullet shaped gas bubble known as "Taylor Bubble" and the unmerged small gas bubbles found in the liquid slug.

Let (t_u) be the time for the slug unit to pass through the fixed cross section ($O'-O'$) and (t_{TB},t_{LS}) be the passing times of the Taylor bubbles and liquid slug respectively (Orell & Rembrand 1986), so :

$$t_u = t_{TB} + t_{LS} \tag{18}$$

Moreover (Abdul-Majeed & Al-Mashat 2000) :

$$t_{TB} = \frac{Z_{TB}}{U_{TB}} \; ; \; t_{LS} = \frac{Z_{LS}}{U_{TB}} \; ; \; t_u = \frac{Z_u}{U_{TB}} \tag{19}$$

During a time (t_u), the volume of the gas (V_g) passing through the ($O'-O'$) equal to the volume of the Taylor bubble plus the volume of the dispersed gas bubbles in the liquid slug Abdul-Majeed & Al-Mashat 2000), so:

$$V_g = V_{g,TB} + V_{g,LS} = \dot{V}_{g,TB}.t_{TB} + \dot{V}_{g,LS}.t_{LS} \tag{20}$$

The void fractions at the Taylor bubble section and at the liquid slug section are given by (Abdul-Majeed & Al-Mashat 2000):

$$\alpha_{TB} = \frac{A_{TB}}{A_{ris}} \; ; \; \alpha_{LS} = \frac{A_{GLS}}{A_{ris}} \tag{21}$$

The volume flow rate of the gas leaving as a Taylor bubble and as dispersed bubbles in the liquid slug are given by (Abdul-Majeed & Al-Mashat 2000):

$$\dot{V}_{g,TB} = U_{TB} A_{TB} = U_{TB} \alpha_{TB} A_{ris} \tag{22}$$

$$\dot{V}_{g,LS} = U_{GLS} A_{GLS} = U_{GLS} \alpha_{LS} A_{ris} \tag{23}$$

Substitute eqs.(19),(22),and (23) in eq.(20), give:

$$V_g = U_{TB} \alpha_{TB} A_{ris} t_{TB} + U_{GLS} \alpha_{LS} A_{ris} t_{LS} = U_{TB} \alpha_{TB} A_{ris} \frac{Z_{TB}}{U_{TB}} + U_{GLS} \alpha_{LS} A_{ris} \frac{Z_{LS}}{U_{TB}} \tag{24}$$

During the unit cell time period, the volume of the gas entering continuously through the section (*O-O*) is (Orell & Rembrand 1986):

$$V_g = \dot{V}_g . t_u = j_g . A_{ris} . \frac{Z_u}{U_{TB}} \quad (25)$$

Equating eq.(24) with (25) and simplify gives:

$$j_g = \beta \alpha_{TB} U_{TB} + (1-\beta)\alpha_{LS} U_{GLS} \quad (26)$$

Where:

$$\beta = \frac{Z_{TB}}{Z_u} = \frac{t_{TB}}{t_u} \quad (27)$$

Liquid Mass Balance:

The mass balance of the liquid phase flowing within the slug unit can be derived following the same approach of the gas mass balance. During the time period (t_{TB}), there is a downward flow of liquid film that rounded the Taylor bubble as it passes through section ($O' - O'$). The resultant continuity equation is (Abdul-Majeed & Al-Mashat 2000):

$$j_L = U_{LS}(1-\alpha_{LS})(1-\beta) - U_{film}\beta(1-\alpha_{TB}) \quad (28)$$

Two-phase Mixture Volume Balance:

Assuming the slug flow is incompressible, the mixture volume balance may be obtained with respect to control surfaces that cut through the liquid slug and Taylor bubble sections. This will result in two equations following the same steps in the gas and liquid mass balance (Orell & Rembrand 1986):

$$j_{tot} = j_g + j_L = U_{GLS} . \alpha_{LS} + U_{LS} . (1-\alpha_{LS}) \quad (29)$$

$$j_{tot} = U_{TB} . \alpha_{TB} - U_{film} . (1-\alpha_{TB}) \quad (30)$$

The four continuity eqs. (26), (28), (29), and (30) do not form a set of independent equations and only three of them are needed to close the model.

Taylor Bubble Rise Velocity:

This is a very important parameter in the slug flow modeling. It represents the translation velocity for the slug unit. Nicklin's et al. (1962) were the first who recognized that the bubble velocity in a flowing liquid is a superimposition of two components as (Collier & Thome 1994):

$$U_{TB} = 1.2\, j_{tot} + U_o \quad (31)$$

White and Beardmore (as sighted in (Wallis, 1969) give a general formula for the rise velocity of the Taylor bubble in a stagnant liquid (U_o) as:

$$U_o = \Gamma \sqrt{(g . D_{ris})} \quad (32)$$

Where:

$$\Gamma = 0.345 \left[1 - Exp\left(-\frac{0.01 N_f}{0.345} \right) \right] * \left[1 - Exp\left(\frac{3.37 - Bo}{\omega} \right) \right] \quad (33)$$

Where:

$$N_f = \sqrt{\frac{\rho_L(\rho_L - \rho_g).g.D_{ris}^{\ 3}}{\mu_L^{\ 2}}} \quad ; \quad Bo = \frac{(\rho_L - \rho_g).g.D_{ris}^{\ 2}}{\sigma_L}$$

$$\omega = 10 \quad when \quad N_f > 250$$

$$\omega = 69(N_f)^{-0.35} \quad when 18 < N_f < 250$$

$$\omega = 25 \quad when \quad N_f < 18$$

The dimensionless inverse viscosity N_f is the ratio between the root of the Froude number and the Reynolds number. For higher values of dimensionless inverse viscosity (usually when N_f>300), the flow is considered inviscid in the liquid near the bubble nose (Wallis, 1969). This assumption applies only when viscosity has a negligible influence. The bubble velocity increases as N_f increases. The Bond number (Bo) is the ratio between the gravity and surface tension forces. For higher values of Bond number (usually when Bo>100), the effect of surface tension will be negligible and this occurs when the pipe diameter satisfies the condition (Wallis, 1969). Increasing Bond number results in higher bubble's velocity.

Slug Bubbles Velocity:

The absolute rise velocity of the dispersed gas bubbles (U_{GLS}) is treated in the same way like the Taylor bubble. Many researchers recommended Harmathy's equation (as sighted in Collier &Thome (1994)) for the rise velocity of dispersed bubbles in a stagnant liquid, so:

$$U_{GLS} = U_{LS} + 1.53\left[\frac{\sigma_L g(\rho_L - \rho_g)}{\rho_L^{\ 2}}\right]^{0.25}(1-\alpha_{LS})^{0.5} \tag{34}$$

The Liquid Film Thickness:

The liquid film thickness (δ) is related to (α_{TB})(Orell & Rembrand 1986) as:

$$\alpha_{TB} = \frac{A_{TB}}{A_{ris}} = \frac{D_{TB}^{\ 2}}{D_{ris}^{\ 2}} = (1 - \frac{2\delta}{D_{ris}})^2 \tag{35}$$

Several methods are found in literature to relate (U_{film}) with (δ). The simple way that is adopted her is given by Orell & Rembrand (1986) which make force balance of the liquid film neglecting the interfacial shear force along the Taylor bubble and assuming no pressure drop across it:

$$\rho_L.g.A_{film}.Z_{TB} = \tau.\pi.D_{ris}.Z_{TB} = (f\frac{1}{2}.\rho_L.U_{film}^{\ 2}).\pi.D_{ris}.Z_{TB} \tag{36}$$

Where friction factor (f) is a function of Reynolds number (based on hydraulic diameter) and pipe roughness (Darby, 2001):

$$\mathrm{Re} = \frac{4.\rho_L.A_{film}.U_{film}}{\pi.D_{ris}.\mu_L} \tag{37}$$

The explicit form for (f) given by the eq. (10) is used.

Liquid Slug Void Fraction:

The basic difficulty in the slug flow modeling is concerned with the gas content in the liquid slug (Orell & Rembrand 1986, Abdul-Majeed & Al-Mashat 2000). In the absence of a predictive method, two limiting cases have been recognized (Orell & Rembrand 1986), namely ideal slug flow (α_{LS}=0) and (α_{LS}=0.3). The latter value represents the upper void fraction limit observed in the bubbly flow. In this study the maximum allowable void fraction is considered since it best describe the real situation.

Slug-Unit Void Fraction:

The slug unit void fraction is defined as the ratio of the gas volume in the Taylor bubble plus the liquid slug sections relative to the slug unit volume. The slug unit void fraction is assumed equal to the riser void fraction according to the principle of cell analysis Orell & Rembrand (1986), hence:

$$\alpha_{tot} = \alpha_{TB}.\beta + \alpha_{LS}(1-\beta) \tag{38}$$

Slip Ratio:

It is the ratio of the gas phase velocity (U_g) to the liquid phase velocity (U_L) (Collier & Thome 1994), i.e:

$$S = U_g / U_L \tag{39}$$

This term could be related to void fraction and dryness fraction(Collier & Thome 1994) as:

$$S = \left(\frac{x}{1-x}\right).\left(\frac{\rho_L}{\rho_g}\right).\left(\frac{1-\alpha}{\alpha}\right) \tag{40}$$

3.RESULTS AND DISCUSSION:

The theoretical equations governing the performance of the bubble pump are solved to obtain the whole pump behavior based on water properties. The solution algorithm is shown in fig.(3) and the computer code is written by Engineering Equation Solver (EES) software. The inputs to the one dimensional slug model are the properties of the phases and the superficial velocities and the main output is the total void fraction. The "By-Section" numerical method was used in the major iteration while the inner iteration was solved by the usual try and errors method.

In the present study, the riser tube length is fixed to 1.5 m while three diameters are tested; 6.5, 10, and 14 mm. The selected submergence ratios are 0.5, 0.6, 0.7, and 0.8.

The Engineering Equation Solver (EES) Software:

The complete modeling for this study was done using the Engineering Equation Solver (EES) software program, which is developed by F-CHART SOFTWARE® (Klein & Alvarado, 2004). The EES is a software package with a built-in thermodynamic and transport property relations of many commonly found substances such as air, water, and most refrigerants. These features makes the EES is a very helpful tool for solving the problems in thermal engineering. In this study, the "Procedure-Call" mode, was used in which one can build his own iteration the logical statement "IF...THEN...ELSE, GOTO, REPEAT-UNTIL….etc" as well as the "FUNCTION" statement to reach the solution all are used.

The Effect of the Heat Input:

The pump discharge characteristic curve in terms of the pumped liquid is obtained as a function of the heat input. Figs. (4,5,6) reveal that for any riser tube diameter and submergence ratio, the mass flow rate of the pumped liquid increases with increasing the amount of the heat input until it reaches a maximum discharge point. Then any further increase in the supplied heat will cause the

liquid mass flow rate to become lower. The physical explanation for this behavior can be attributed to the increase in the frictional pressure drop due to the increase in the vapor mass flow and due to the expected change in the flow pattern from slug to mainly annular shape, this explanation coincides with the explanation of Delano (1998), Sathe (2001), and Shihab et al. (2012). In the annular flow pattern, the liquid dragged up mainly by the action of shear stress between high velocity vapor and the liquid and partially by the buoyancy action at which condition the slip ratio is too high. When the heat input is lower than the optimum point, the vapor buoyancy effect still has the ability to overcome the additional frictional pressure drop. This ability appears in a further increase in the pumped liquid up to the maximum point.

Fig.(7) shows comparison between the results of the present analytical model and Faisal's (2012) experimental results the pumping capacity for water input temperature to the generator of 102 °C and for 10 mm riser tube diameter. This figure indicates that the theoretical results have a comparable trend in their variation with that obtained experimentally by Faisal. This comparison verified the applicability of the present model to describe the bubble pump behavior.

It can be mentioned her that the generated amount of vapor is linear related to the amount of heat supplied at the generator as long as the supplied water is saturated as shown in fig.(8). In this case the variation of vapor mass flow rate will be independent of the submergence ratio. This behavior is mainly due to the latent heat of vaporization. This property is almost constant within the selected submergence ratios.

The variation of pumping ratio (the ratio of volume flow rate of the pumped liquid to volume flow rate of the vapor), with the heat input for a given pump tube diameters and different submergence ratio are illustrated in Figs. (9, 10, and 11). The pumping ratio which may consider as an indicator of the pumping efficiency decreases with the increase in heat input for all diameters and submergence ratios. This is due to the increase of vapor flow rate and the consequently increase in pressure head loss. It is noticed that the pumping ratio increases with the increase of the pump tube diameter with the same amount of heat supply. Bigger the diameter, smaller is the pressure drop and higher is the mass flow of the pumped liquid then higher is the liquid pumping rate.

Effect of Generator Inlet Temperature:

Fig.(12) shows clearly that the maximum pumping capacity is independent of the liquid temperature entering the generator, it is only need more heat for the sensible heating prior to the evaporation. This fact is true for any tested submergence ratio. Therefore, the whole pumping characteristic curve is merely shifted to a higher heat input point with the same maximum pumping capacity. According to this fact, it is useful to draw the discharge characteristics with respect to the submergence ratio instead of heat input and confine the attention to the maximum pumping capacity point.

Effect of the Submergence Ratio:

Referring again to Figs.(3,4,5), they show also how the pumping capacity varies positively with the increasing of submergence ratio. They reveals that for any riser tube diameter, an increase in the submergence ratio (and thereby the driving head), leads to an increase in the maximum liquid discharge associated with a decrease in the optimum vapor mass flow rate. These facts are represented clearly in the figs.(13, 14). The main causes of this behavior are due to the decrease in the pump lift (L_{ris}-Z_d) and the increasing of the driving head relative to a fixed riser tube height. For

the 10 mm tube diameter, the increase in the submergence ratio from 0.5 to 0.8 causes the pumping capacity to increase from 0.0316 to 0.0564 kg/s, i.e., a percent increase of 78.5%. Fig.(14) shows clearly that the optimum vapor flow rate decreases as the submergence ratio increases. This behavior is occurring mainly due to the increase in the driving head as well as due to the increase in the saturation temperature. Increasing the temperature leads to reduce the gravitational force and make the fluid to be less viscous which leads to less frictional force. All these effects make the

pumping process easier and attributes smaller amount of vapor to overcome the flow restrictions. For example, using the 10mm tube diameter, the increase in the submergence ratio from 0.5 to 0.8 causes the vapor flow rate to decrease from 0.0835 to 0.0635 g/s, i.e., a percent decrease of 24%.

Effect of the Riser Diameter:

Examining fig.(13) explains that the maximum pumping capacity of the bubble pump with larger tube diameter is higher than that of the smaller diameter. That fact comes from the lowering of the frictional pressure drop when using larger tube. However, the larger pumping capacity requires a higher amount of vapor mass flow rate that necessary to produce a larger bubble that could occupy the tube cross section and to lift the increasing trapped liquid. For example, at a submergence ratio of 0.6, the increase in the tube diameter from 6.5 to 10 will cause the pumping capacity to increase by 223%. Further increase to 14 mm will increase this percent to 646%. However, the larger tube requires a higher heat input that conjugate with a higher mount of vapor generation.

Variation of the Slip Ratio:

Fig.(15) shows how the slip ratio at the optimum pumping point varies with the submergence ratio. The slip ratio is a direct result from the slug model that describes the void fraction in the riser tube at any time. The figure reveals that the slip ratio deceases as the submergence ratio increases. This behavior is due to the decrees in pump's lift as the submergence ratio increases which requires a lower vapor mass flow rate (and thereby lower vapor velocity) relative to the water velocity. The figure also demonstrates that the slip ratio decreases as the riser tube diameter decreases which is a direct result from the lowering of the required optimum vapor mass flow rate and thereby lower vapor velocity. The slip ratio varies approximately from 1.44 to 2.15 for the selected submergence ratios and tube diameters.

4.CONCLUSIONS:

From the discussed results, the following conclusions are drawn:

1. The thermal bubble pump of a given diameter, submergence ratio, and length has a limited maximum pumping capacity at a specified vapor mass flow rate.
2. The maximum pumping capacity of the thermal bubble pump is found to be independent of the liquid temperature at the inlet to the generator, while it is positively affected when both the submergence ratio and riser tube diameter are increased.
3. The optimum vapor mass flow rate decrease as submergence ratio increase and increases with increasing tube diameter.
4. The slip ratio decrease as submergence ratio increases and it slightly increase with increase the tube diameter.

RECOMMENDATION:

It is strongly recommended to verify the mathematical model with experimental data.

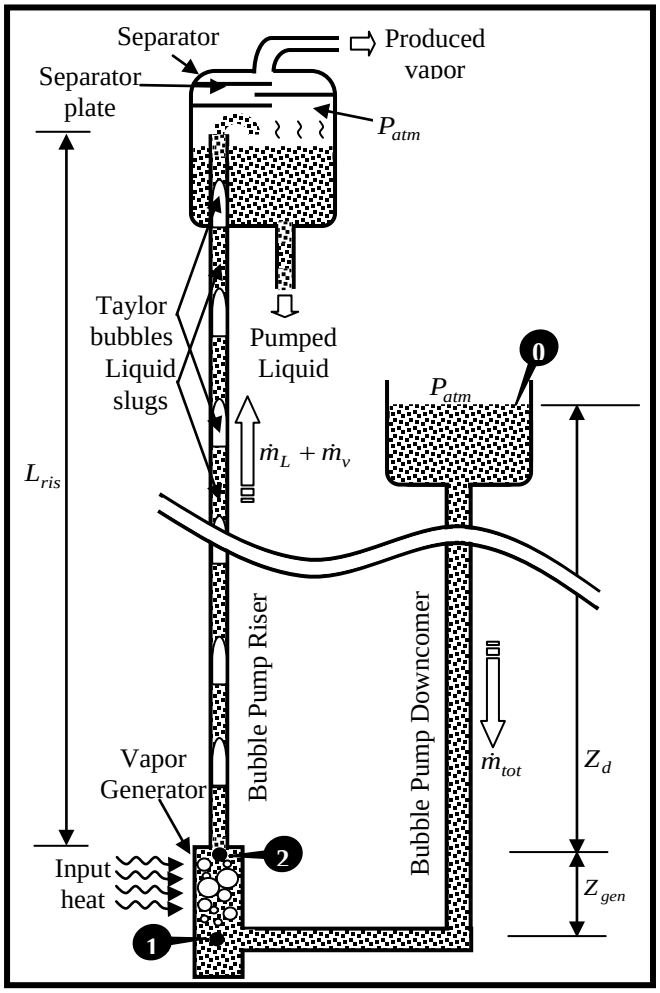

Fig.1 Schematic of the water-based thermal bubble pump.

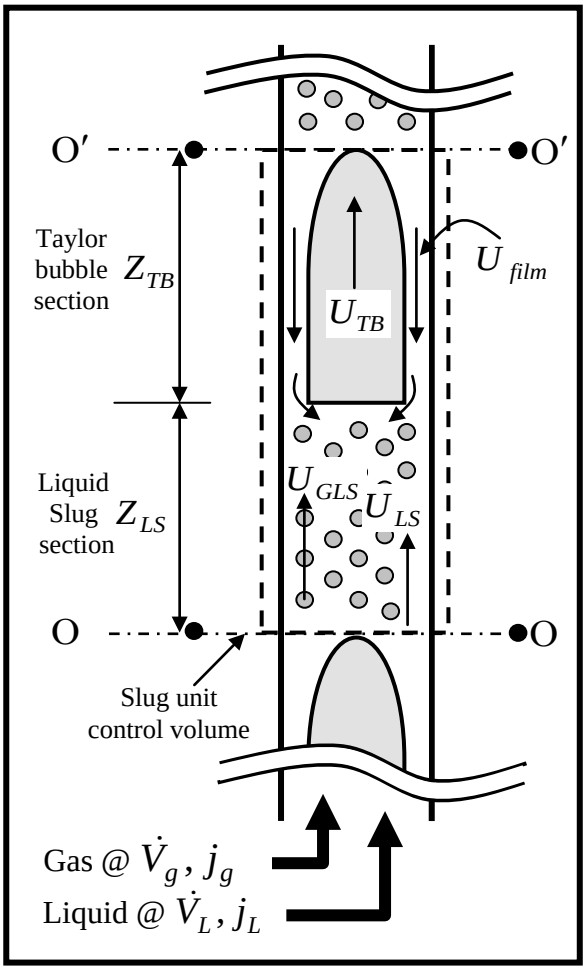

Fig.2 One-dimensional model for slug flow along the riser tube.

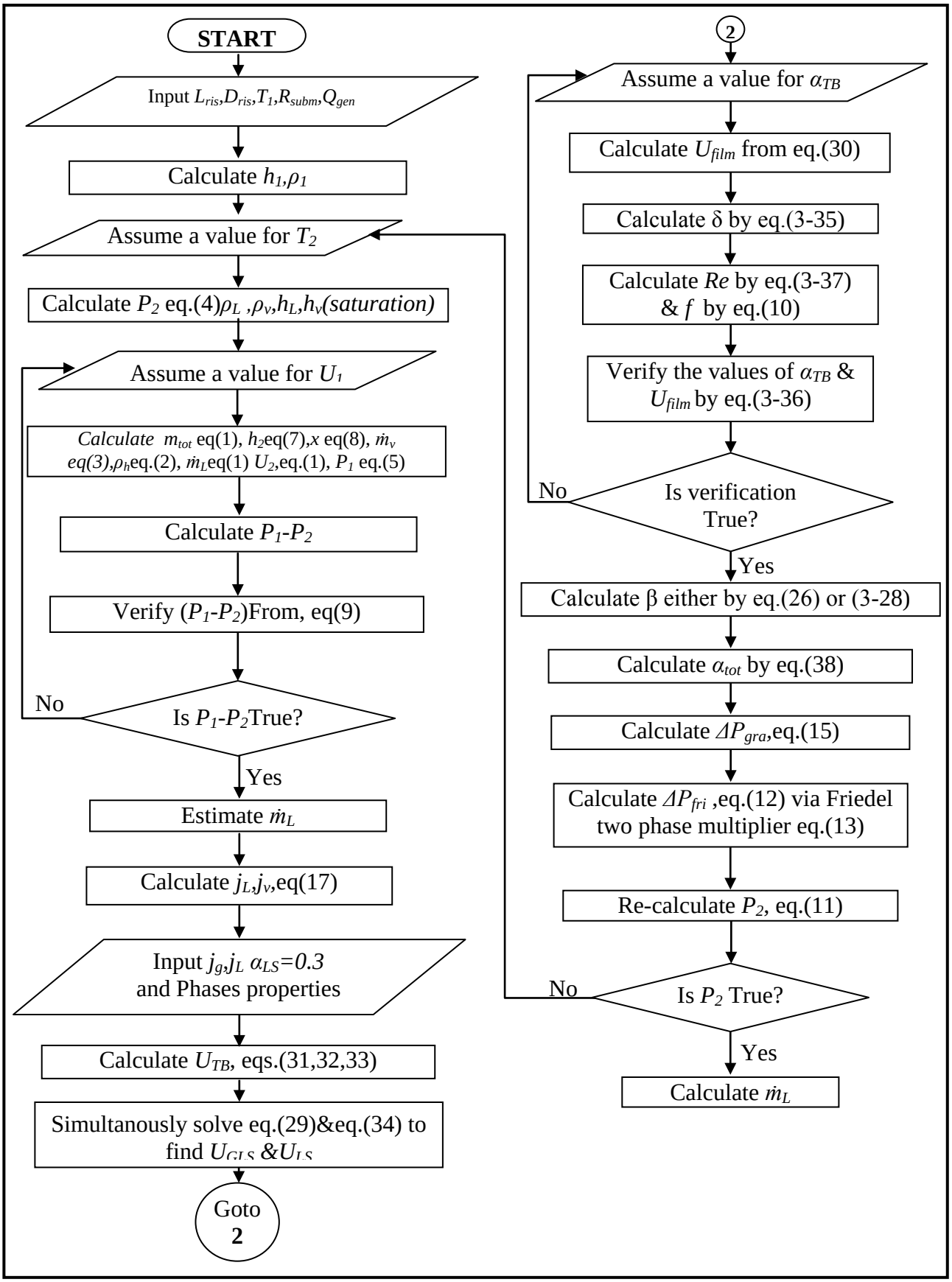

Fig.3 Flow Chart for the for solution method of the analytical model.

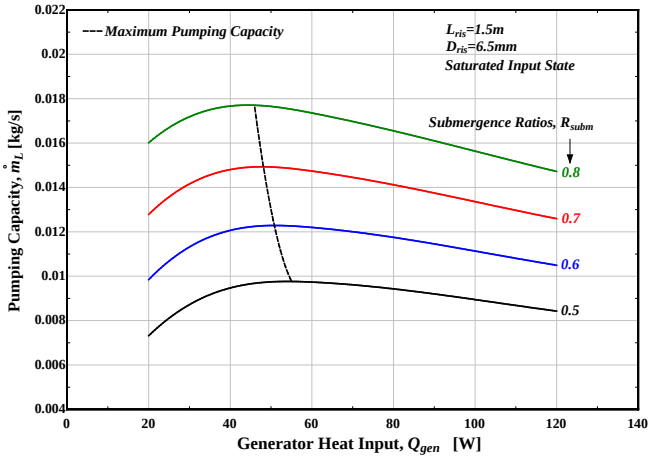

Fig.4 Variation of pumping capacity with generator heat input for D_{ris}=6.5mm.

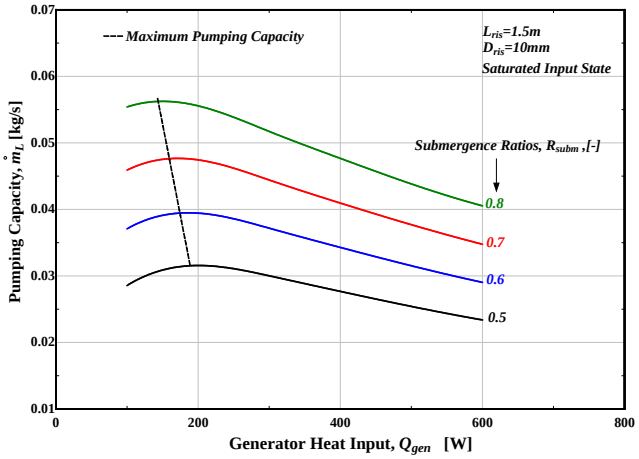

Fig.5 Variation of pumping capacity with generator heat input for D_{ris}=10mm.

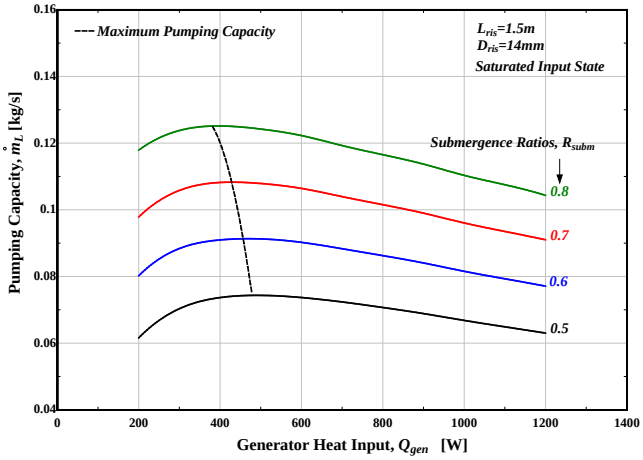

Fig.6 Variation of pumping capacity with generator heat input for D_{ris}=14mm.

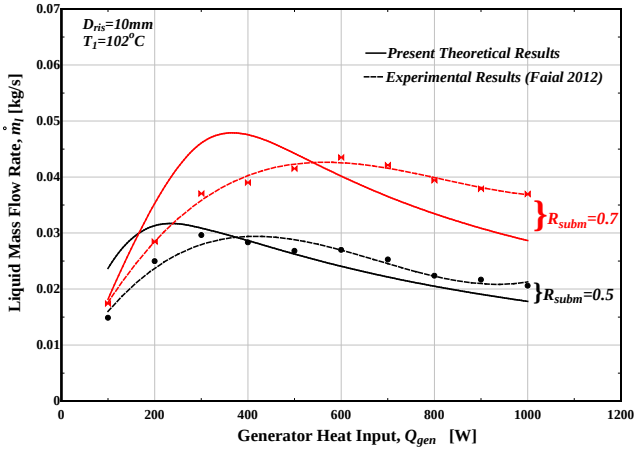

Fig.7 Comparison of predicted pumping capacity behavior with experimental results

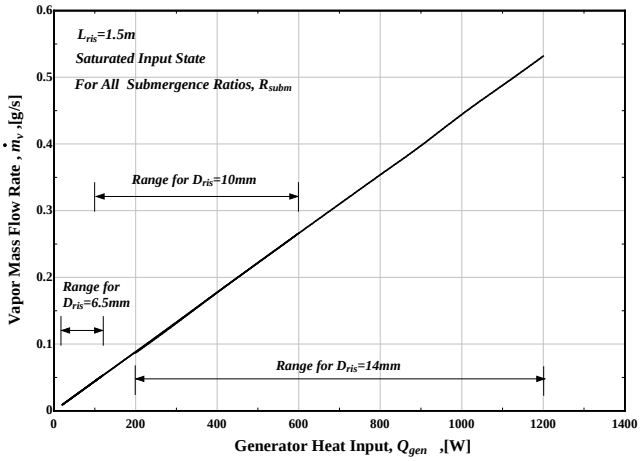

Fig.8 Variation of vapour flow rate with generator heat input using different riser diameters.

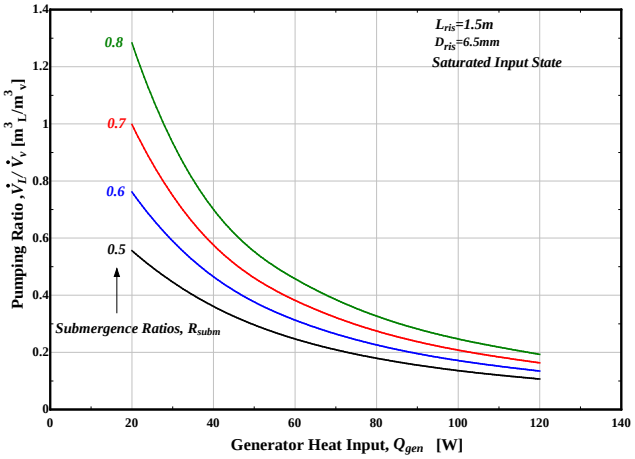

Fig.9 Variation of pumping ratio with generator heat input for D_{ris}=6.5mm.

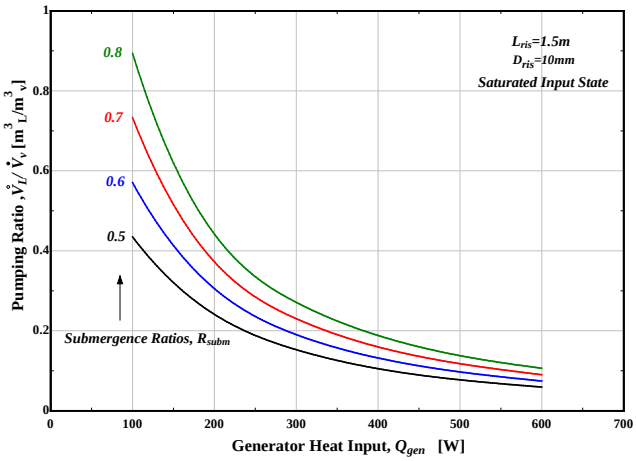

Fig.10 Variation of pumping ratio with generator heat input for D_{ris}=10mm.

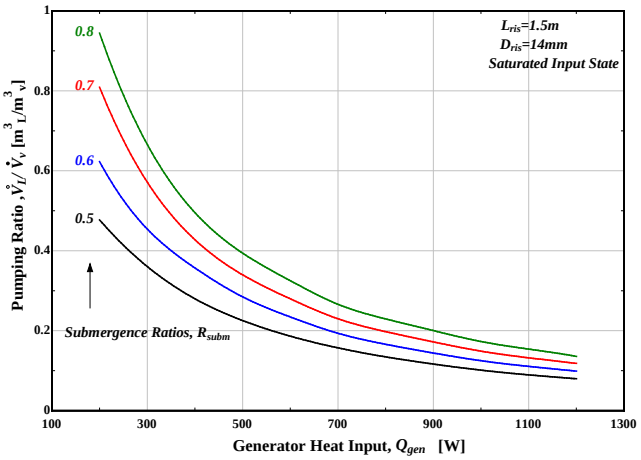

Fig.11 Variation of pumping ratio with generator heat input for D_{ris}=14mm.

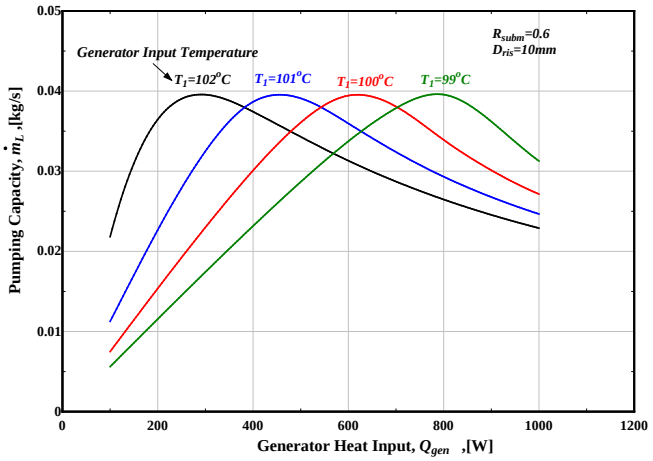

Fig.12 Variation of pumping capacity with generator heat input using different input temperatures for the generator.

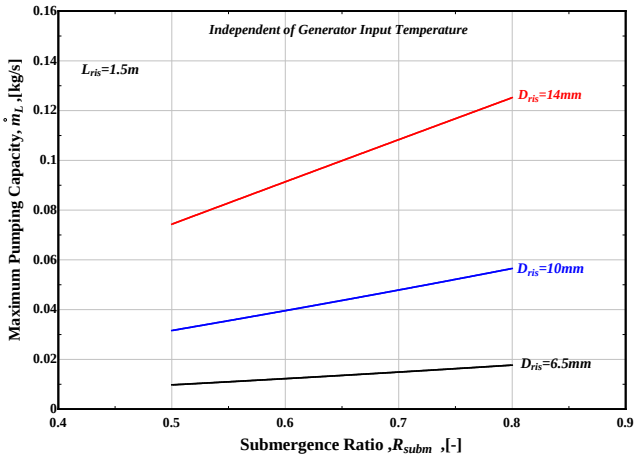

Fig.13 Variation of maximum pumping capacity with submergence ratio using different riser diameters.

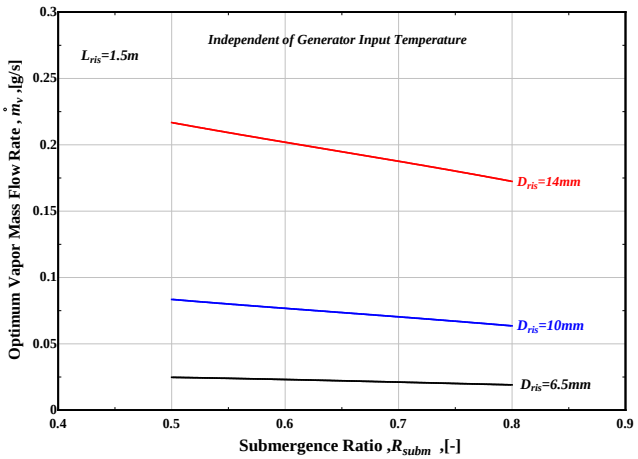

Fig.14 Variation of optimum vapour flow rate with submergence ratio using different riser diameters .

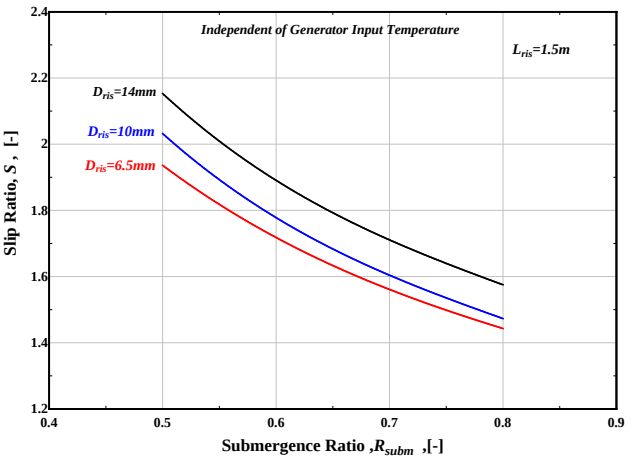

Fig.15 Variation of slip ratio at the optimum pumping point with submergence ratio using different riser diameters .

REFERENCES:

Abdul-Majeed, G.H, & Al-Mashat, A.M, "A Mechanistic Model for Vertical and Inclined Two-Phase Slug Flow", Journal of Petroleum Science and Engineering, Vol.27, pp.59–67, 2000.

Collier, J.G, & Thome, J.R, "Convective Boiling and Condensation", 3rd ed., Oxford University Press Inc., N.Y, 1994.

Darby, R., "Chemical Engineering Fluid Mechanics",2nd ed., Marcel Dekker, Inc., 2001.

Delano, A.D, "Design Analysis of the Einstein Refrigeration Cycle", PhD Dissertation, Georgia Institute of Technology, Georgia, U.S.A, 1998.

Faisal, S.H, " Performance Study of LiBr-Water Pumpless Absorption Refrigeration System", PhD Dissertation, University of Basah, Basrah , Iraq, 2012.

Klein, S.A & Alvarado, F.L, "Engineering Equation Solver-EES Software", F-Chart Software®, Professional-Ver.7.124, 2004.

Koyfman, A., Jelinek, M., Levy, A. & Borde, I., "An Experimental Investigation of Bubble Pump Performance For Diffusion Absorption Refrigeration System With Organic Working Fluids", Applied Thermal Engineering, Vol.23, pp.1881-1894, 2003.

Orell, A., & Rembrand, R.," A Model for Gas –Liquid Slug Flow in a Vertical Tube", Trans. ACS, Ind.Eng.Chem.Funda,Vol.25,No.2, pp.196-206, 1986.

Pfaff, M., Saravanan, R., Maiya, M.P, & Murthy, S.S, " Studies on Bubble Pump for A water-Lithium Bromide Vapour Absorption Refrigerator", Int.J. Refrigeration, Vol.21, No.6, pp.452-562, 1998.

Sathe, A.,"Experimental and Theoretical Studies on a Bubble Pump for a Diffusion Absorption Refrigeration System", M.Sc thesis, Indian Institute of Technology, Madras, 2001.

Shihab, A.W.S, Morad, A.M.A, "Experimental Investigation of Water Vapor-Bubble Pump Characteristics and its Mathematical Model Reconstruction", Engineering & Technology Journal, Vol. 30, No.11, 2012.

Stenning, A., & Martin, C., "An Analytical and Experimental Study of Air-Lift Pump Performance", Trans. ASME, Journal of Engineering for Power, Vol.90, No.2, pp.106-110, 1968.

Vicatos, G., & Bennett, A., "Multiple Lift Tube Pumps Boost Refrigeration Capacity in Absorption Plants", Journal of Energy in South Africa, Vol.18, No.3, 2007.

Wallis, G. B., "One-Dimensional Two Phase Flow", McGraw-Hill Companies, Inc., N.Y, 1969

Zhang, L., Wua, Y. , Zheng, H. , Guoa, J. , & Chena, D. ,"An Experimental Investigation on Performance of Bubble Pump with Lunate Channel for Absorption Refrigeration System", Int.J.of Refrigeration, Vol.29, pp.815–822, 2006.